Clays and Clay Minerals, Vol. 48, No. 1, 1–9, 2000.

STRUCTURAL MODEL OF Al_{13}-PILLARED MONTMORILLONITE

VIRGIL I. DIMOV, ALBENA V. ILIEVA, NELLY G. KHALTAKOVA, AND LIUDMILA D. FILIZOVA
Central Laboratory of Mineralogy and Crystallography, Bulgarian Academy of Sciences, 1000 Sofia, Bulgaria

Abstract—Alumina-pillared montmorillonite is prepared by intercalation of polyoxyhydroxy aluminum cations (Al_{13}^{7+}) of a natural montmorillonite from Dimitrovgrad, Bulgaria. Transmission electron microscopy, powder X-ray diffraction, energy dispersive X-ray spectroscopy, and surface area (BET) methods are used to study the untreated and pillared forms of the montmorillonite. A structural model involving deformed Al_{13} pillars is proposed. Four pillar types are derived and these pillars are uniformly distributed over the interlayer-cation positions of montmorillonite. Calculated electron diffraction patterns were simulated using the multi-slice method. The structural model explains the increased ordering along the *c* axis of the pillared form compared with the untreated montmorillonite. The model explains the structure of a pillared montmorillonite with different distributions of the pillars in the interlayer. The proposed model is consistent with the observed data.

Key Words—Alumina Pillaring, Computer Simulation, Keggin Pillaring, Montmorillonite, Structural Model, Transmission Electron Microscopy.

INTRODUCTION

The intercalation of large complexes with high positive charge in the interlayer of smectite, whose structural 2:1 layers have a relatively low negative charge, produces structures with a two-dimensional system of micropores between 0.6–2.0 nm in size. The stability of these modified layer structures depends on many factors, such as the chemical and structural nature of the host matrix (particle size, layer-charge distribution, type of interlayer-cation complex, *etc.*), the homogeneity of the pillaring agent solutions, and the bonds between the host matrix and the pillars. These factors were studied previously (*e.g.,* Pinnavaia, 1983; Plee *et al.,* 1987; Vaughan and Lussier, 1980), but the structural changes arising in the "pillaring" process were not entirely clarified (Vaughan, 1988).

Al-pillared smectites are the most studied clay minerals in this respect (Schoonheydt, 1994). An increase in the degree of ordering of the smectite 2:1 layers along the *c* axis owing to the pillaring process was observed by Schoonheydt (1994) and Figueras *et al.* (1990). The layers "aggregate", forming so-called "tactoids", with every two adjacent layers predominantly oriented face-to-face and with an observed *d*(001) of the newly formed structure at ~18 Å. High-charged Ca-rich montmorillonites of relatively higher degree of crystallinity were found to form such tactoids (Schoonheydt, 1994). The important role of the crystal-chemical properties of the clay matrix was discussed by Occelli *et al.* (1987) and Fijal and Klapyta (1993).

The purpose of this paper is to propose a structural model of Al_{13}-pillared montmorillonite. The model is based on literature data and on a comparative investigation using transmission electron microscopy (TEM) of a natural Ca-rich montmorillonite of low-iron content and relatively high layer charge and its Al_{13}-pillared analogue. The validity of the model is tested by comparing observed TEM patterns with microdiffraction patterns of modeled pillared structures simulated using the multi-slice method.

MATERIALS AND METHODS

Montmorillonite (<2-μm fraction), separated from a white Ca-rich bentonite clay, Dimitrovgrad region, southern Bulgaria, was used as starting material. The fraction studied was separated by sedimentation and contains montmorillonite (~60%), cristobalite (~30%), and calcite (~10%) as determined by powder X-ray diffraction (XRD).

A portion of the sample was used to prepare pillared-montmorillonite samples using the procedure of Schönherr *et al.* (1981). The pillaring solution containing $[Al_{13}O_4(OH)_{24}(H_2O)_{12}]^{7+}$ cations was obtained by adding 0.25 M NaOH solution to a 0.25 M $AlCl_3{\cdot}6H_2O$ solution and aging for 3 h at room temperature. The resultant solution of pH = 4.5 and OH/Al ratio of 2.0 was added to the clay suspension (1 g clay/200 mL H_2O) and stirred for 3 h at 80°C. The pillared form was then centrifuged, filtered, and dried at 60°C in air. Calcination was performed at 500°C. The degree of intercalation of the pillaring cations was determined by XRD, by analyzing variations of *d*(001) in oriented clay-aggregate specimens. A DRON UM1 powder diffractometer with CuKα radiation and a Ni filter was used.

Another portion of the sample was treated (Foster, 1953) to remove cristobalite. The chemical composition of this sample, the untreated sample, and the pillared product was studied by energy dispersive X-ray analysis (EDX) in a raster mode on pressed tablets at an acceleration voltage of 18 kV using a Philips 515 scanning electron microscope (SEM), equipped with

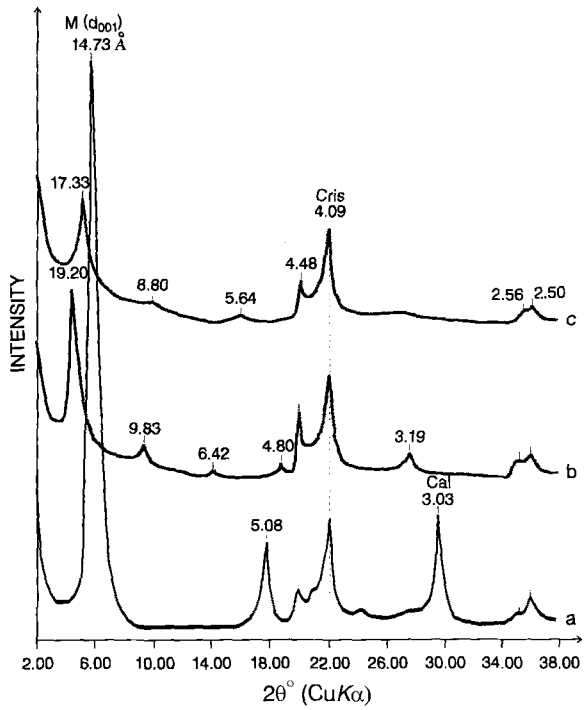

Figure 1. Powder XRD patterns of a) natural, b) intercalated, and c) calcined montmorillonite.

an EDAX 9100/70 system. Biotite, albite, anhydrite, and rutile were used as reference standards.

The chemical-composition data were used to obtain the structural formula of the pure, non-pillared montmorillonite and to calculate the ratio: $Si_{Mont.}/Si_{Total}$, where $Si_{Mont.}$ is the Si content in the montmorillonite and Si_{Total} is the Si content in the starting material. Using this ratio, the quantity of Al_{13}-pillaring cations intercalated in montmorillonite was calculated.

Specific surface areas of the natural and pillared samples were calculated by the BET method using N_2-adsorption data obtained by a Micromeritics ASAP 2010 surface area analyzer. Electron microscopy was performed on a TEM Philips EM 420 at an accelerating voltage of 80 kV. The samples were prepared by using ultrasonically pretreated suspensions of the material on a holey carbon film on a Cu grid. Calculated single-crystal diffraction patterns from model structures of montmorillonite, with and without pillars, were obtained using a custom computer program based on the multi-slice method of Cowley and Moodie (1957).

Structural models of montmorillonite pillared by polymeric Al_{13} cations were prepared using the following steps: (a) development of a hypothetical structural model of natural montmorillonite, ordered along the *c* axis; (b) modification of this ordered hypothetical structure by enlargement of the interlayer distance (hereafter referred to as an "enlarged-interlayer montmorillonite"); (c) modeling of the Al_{13} pillar; and (d) arrangement of the pillars between the layers of the enlarged-interlayer montmorillonite structure. Simulated electron diffraction patterns (EDP) of the models of the pillared montmorillonite were compared to patterns from the enlarged-interlayer montmorillonite and each was compared to the experimental EDP of the pillared montmorillonite.

Table 1. Chemical composition of the natural and pillared samples. 1) fraction <2 μm of Dimitrovgrad bentonite – untreated; 2) fraction <2 μm treated with NaOH to dissolve cristobalite; 3) Al_{13}-pillared sample.

Oxides, wt. %	1	2	3
SiO_2	70.75	54.91	58.80
Al_2O_3	13.08	19.02	20.05
Fe_2O_3	0.93	1.50	0.88
MgO	1.77	3.14	2.18
CaO	3.47	7.40	0.10
Na_2O	—	0.72	0.64
K_2O	0.22	0.39	0.30

RESULTS

The observed values of $d(001)$ for untreated, intercalated, and calcined samples from XRD (Figure 1) are 14.73, 19.20, and 17.33 Å, respectively. The value of $d(001) = c\sin\beta = 17.33$ Å corresponds to a value for c of 17.68 Å for $\beta = 101.4°$ (see below) for the pillared montmorillonite considered in the model construction.

The chemical compositions of the natural, NaOH-treated, and pillared samples are given in Table 1. The structural formula of the montmorillonite $Na_{0.10}K_{0.04}Ca_{0.12}(Si_{3.96}Al_{0.04})_4(Al_{1.58}Mg_{0.34}Fe^{3+}_{0.08})_2O_{10}(OH)_2$ was calculated after dissolving cristobalite and analyzing the cristobalite-free fraction (Table 1, column 2). The total charge of the interlayer cations is 0.38, which corresponds to the mean value of the negative layer charge of 0.36 eq/$O_{10}(OH)_2$ obtained from a previous investigation of the same sample by the n-alkylammonium method (Ilieva, 1996). The specific surface area of 65 m^2g^{-1} was measured for the natural sample and 165 m^2g^{-1} for the pillared sample. The results obtained by XRD, EDX, and BET suggest that the pillaring process was complete. From Table 1, a value of 0.516 was determined for the $Si_{Mont.}/Si_{Total}$ ratio. From this ratio and the chemical data of the pillared material (Table 1) one Al_{13} cation is present in 4.2 montmorillonite unit cells.

Figure 2 shows the selected area electron diffraction (SAED) patterns along the [001]* zone axis of the natural and pillared montmorillonite. The SAED patterns of the natural sample (Figure 2a) are polycrystalline owing to turbostratic disorder of 2:1 layers along the *c* axis (Brindley, 1980). The layers are thus randomly superposed, rotated, and/or displaced from

https://doi.org/10.1346/CCMN.2000.0480101 Published online by Cambridge University Press

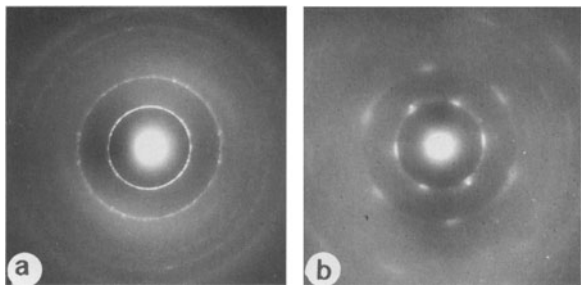

Figure 2. SAED patterns along [001]* zone axis of montmorillonite particles for a) natural and b) pillared samples.

adjacent layers parallel to the *a* and *b* axes. This is a characteristic feature of fine-grained smectite minerals and especially of montmorillonite.

After intercalation of Al_{13} cations, this turbostratic disorder significantly decreased. The SAED patterns have a greater single-crystal character with diffuse maxima (Figure 2b). The additional ordering along the *c* axis is probably caused by the alignment of both the pillars and the 2:1 layers.

ATOMIC MODEL OF Al_{13}-PILLARED MONTMORILLONITE

Model of 2:1 layer and stacking along the c axis

The model of the 2:1 layer of montmorillonite is based on *C2/m* space group symmetry and unit-cell parameters: a = 5.18 Å, b = 8.98 Å, c = 10 Å, α = 90°, β = 101.4°, γ = 90° (model 3 of Tsipursky and Drits, 1984). In this model, *trans-* and *cis-* octahedral sites are occupied with equal probabilities: 75% of both sites are occupied by Mg, Fe, or Al, which corresponds to the elements in the Dimitrovgrad montmorillonite.

Stacking of component parts along the *c* axis was modeled by arranging the 2:1 layers to preserve the *C2/m* symmetry, thus, each 2:1 layer has coinciding [001] directions and *a* and *b* axes. For simplicity, *y* and *z* coordinates (Tsipursky and Drits, 1984) were shifted by 0.5, so that the interlayer cation positions have *xyz* coordinates of 0, 0, 0.5 and 0.5, 0.5, 0.5 (Table 2a).

Model of enlarged-interlayer montmorillonite

The value of c = 17.68 Å of the pillared montmorillonite involved an increase of $d(001)$ owing to adjacent 2:1 layers separating to produce an enlargement of the interlayer. The stacking order and *C2/m* symmetry were retained, assuming the shift is strictly in the [001] direction. Therefore, only the *z* coordinates of the atoms in the 2:1 layer were adjusted in the model (Table 2a). The interlayer cation sites are vacant.

Model of the Al_{13} pillar

The polymeric Al oxy-hydroxy ion (Johansson, 1960; Bottero *et al.,* 1980) is comprised of 12 octahedra and one tetrahedron, all containing Al. The structure of the Al_{13} polycation after intercalation in the clay matrix and after alteration by heating is problematic. Transformations of the pillar occur upon dehydration and dehydroxylation (between 300–400°C), but nuclear magnetic resonance (NMR) studies show that the ^{IV}Al coordination is resistant to change by thermal treatment (Fripiat, 1988; Tilak *et al.,* 1986). Based on thermal gravimetric analysis (TGA) and XRD studies, Kodama and Singh (1989) suggested that Al_{13} pillars dehydrate and dehydroxylate without substantial change in the structure.

A slightly deformed Keggin-ion structure is used here as a model. This ion has three parallel layers consisting of six octahedra in the lower layer, three in the middle layer around a central tetrahedron, and three octahedra in the upper layer. Only Al atoms forming three parallel planes (Figure 3) are considered in the model. This simplification is justified because oxygen atoms scatter electrons weakly and excluding them

Table 2a. Derived atomic coordinates for Al_{13}-pillared montmorillonite. Symmetrically independent atoms of the 2:1 layer (Model 3 of Tsipursky and Drits, 1984). Space group: *C2/m*; lattice parameters: a = 5.18 Å, b = 8.98 Å, c = 10 Å, α = 90°, β = 101.4°, γ = 90°. The origin of the coordinate axes is shifted by $y = y + 0.5$ and the z coordinates are shifted by $z = z + 0.5$ and are recalculated for c = 17.6798 Å.

Sites		Coordinates			Occupancy	
		x	*y*	*z*		
M1	2b	0.0000	0.5000	0.0000	Al	0.5000
					Mg	0.1900
					Fe	0.0700
M2	4g	0.0000	0.8330	0.0000	Al	0.5000
					Mg	0.1900
					Fe	0.0700
T2	8j	0.4270	0.1670	0.1529	Si	0.9400
					Al	0.0600
O1	4i	0.4870	0.0000	0.1865	O	1.0000
O3	8j	0.1720	0.7720	0.1865	O	1.0000
O4	4i	0.3690	0.5000	0.0615	O	1.0000
O6	8j	0.3690	0.8330	0.0615	O	1.0000

Table 2b. Derived atomic coordinates for Al_{13}-pillared montmorillonite. Calculated coordinates of symmetrically independent positions of the pillar Al atoms according to the proposed structural model.

Sites		Coordinates			Occupancy		
		x	*y*	*z*	OVO	OVVO	OVVVO
Al1	8j	0.0966	0.3510	0.3481	0.1250	0.05(5)	0.0312
Al2	8j	0.9926	0.3510	0.3481	0.1250	0.05(5)	0.0312
Al3	8j	0.5446	0.7890	0.3481	0.1250	0.05(5)	0.0312
Al4	8j	0.2856	0.4140	0.3481	0.0625	0.02(7)	0.0156
Al5	8j	0.8036	0.4140	0.3481	0.0625	0.02(7)	0.0156
Al6	8j	0.5446	0.6730	0.3481	0.0625	0.02(7)	0.0156
Al7	2c	0.5000	0.5000	0.5000	0.2500	0.11(1)	0.0625
Al8	8j	0.0520	0.6490	0.5000	0.1250	0.05(5)	0.0312
Al9	4h	0.5000	0.2020	0.5000	0.1250	0.05(5)	0.0312

https://doi.org/10.1346/CCMN.2000.0480101 Published online by Cambridge University Press

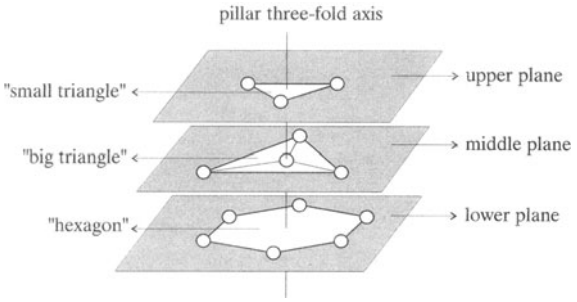

Figure 3. Schematic representation of the Al_{13}-pillaring cation.

from the model does not substantially influence the simulated EDP. The six Al atoms in the lower plane form a hexagon. A triangle is formed by three Al atoms in the middle plane, with each Al positioned directly above three Al atoms of the hexagon as shown in Figure 3. The central Al atom in the middle plane is central also to the pillar. Three Al atoms in the upper plane form an equilateral triangle, but smaller in size, than the triangle of the middle plane. This triangle is centered above the middle plane but rotated by 180°. We refer to the triangles in the middle and upper planes as "big" and "small" triangles, respectively. The model is "orthogonal", because the three-fold axis (Figure 3) is perpendicular to the layer planes, and this model is labeled "primary" or "P".

Pillar configuration in the interlayer

The pillar is positioned in the interlayer between adjacent 2:1 layers (Figure 4) using the following assumptions: (a) the three-fold axis of the pillar is parallel to the normal of the (001) plane of the 2:1 layer (Figure 4a); (b) the Al hexagon of the lower plane of the pillar is placed above a ditrigonal silicate ring of the 2:1 layer (Figure 4b); (c) the lower and upper-pillar

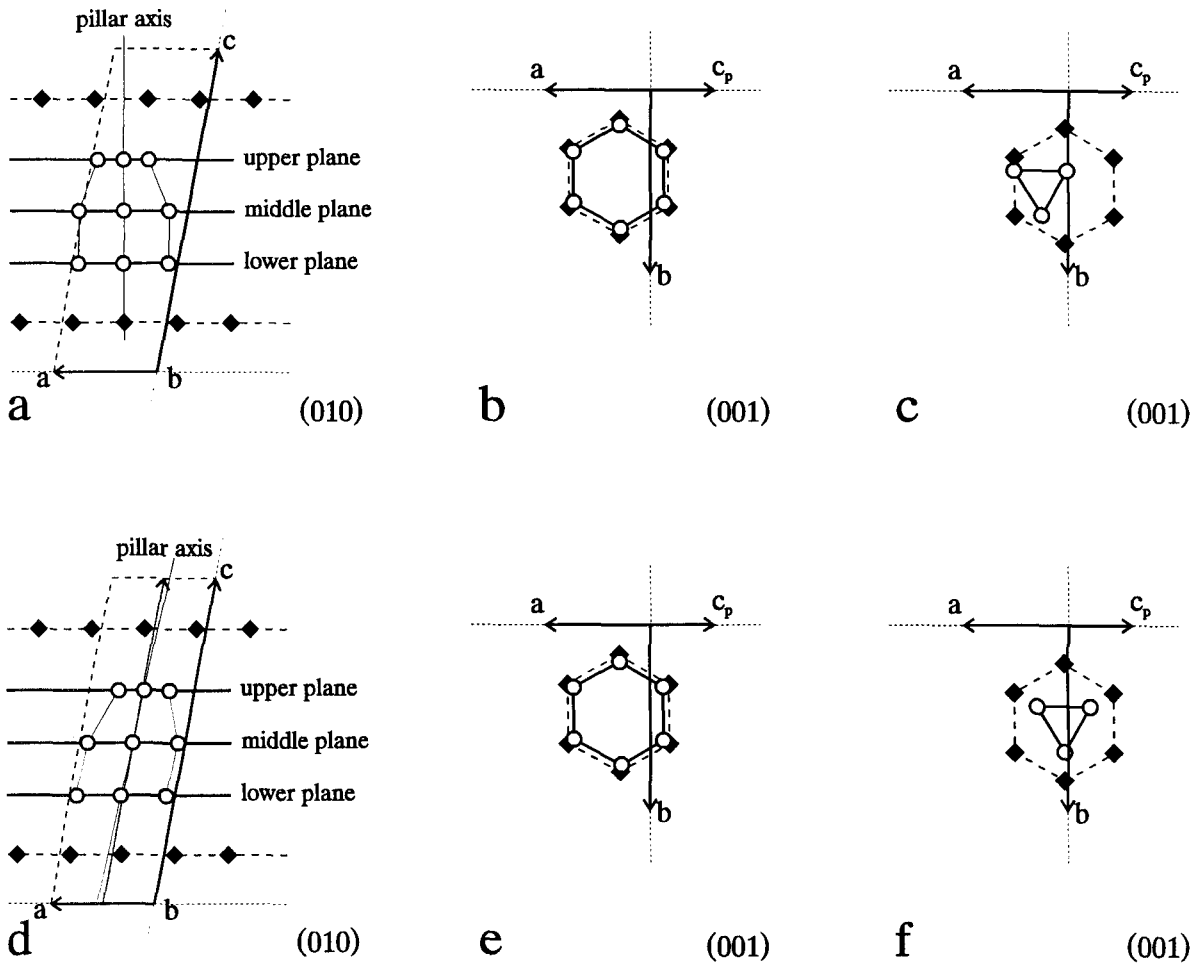

Figure 4. a) (010) projection of the orthogonal pillar and the adjacent Si planes; b) (001) projection of the lower plane of the orthogonal pillar and the Si plane; c) (001) projection of the upper plane of the orthogonal pillar and the Si plane; d) (010) projection of the deformed pillar and the adjacent Si plane; e) (001) projection of the lower plane of the deformed pillar and the Si plane; f) (001) projection of the upper plane of the deformed pillar and the Si plane; ♦ - Si, ○ - Al.

https://doi.org/10.1346/CCMN.2000.0480101 Published online by Cambridge University Press

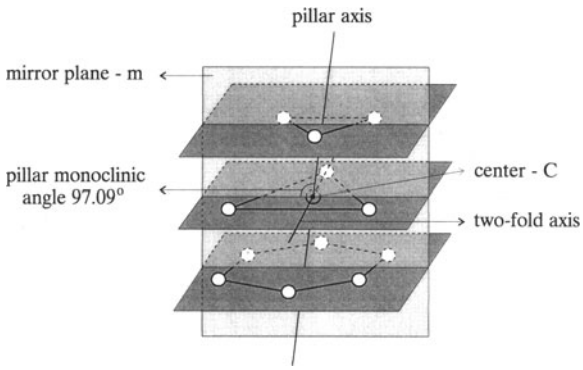

Figure 5. Schematic representation of the deformed Al_{13}-pillaring cation and the symmetry elements of *C2/m* space group.

planes are at an equal distance from adjacent 2:1 layers (Figure 4a).

Figure 4a and 4c shows that the orthogonal Al pillar, when placed in the interlayer in this way, does not conform to *C2/m* symmetry, and an additional assumption is required: the Al triangle of the upper-pillar plane must be placed below the ditrigonal silicate ring of the adjacent 2:1 layer. Thus, the pillar axis inclines and the orthogonal pillar (orthogonal P) is deformed (deformed P) to conform to the *c* parameter (see below). Figure 4d–4f shows projections of the deformed P pillar on the (010) and (001) planes when the pillar is placed above and below a ditrigonal silicate ring of the adjacent 2:1 layers, respectively. This configuration requires the central Al atom of the pillar to occupy the interlayer "cation" position at either (0.5, 0.5, 0.5), or (0, 0, 0.5).

Additional site-symmetry requirements to conform to *C2/m* symmetry (*i.e.*, 2, *m*, $\bar{1}$) must be applied to the deformed P pillar with the central Al atom at the interlayer-cation position (Figure 5). Thus, three possible pillars are generated, referred respectively as "rotated" (R), "mirror" (M), and "centrally inverted" (C) (Figure 6). All four pillars must be present with equal probability in the structure to retain overall *C2/m* symmetry. Each pillar type is configured differently in the interlayer.

The angle of the deformed (P, R, M, or C) pillar is not identical with the β parameter of the overall structure and depends on the *c* parameter. Simple geometric considerations show that the angle of the pillar increases from 90° to 97.4°, if *c* increases from 10.05 to 18.532 Å. For c = 18.532 Å, the upper 2:1 layer is placed above the lower 2:1 layer in the same position as the case where c = 10.05 Å and the angle is 90°. For our model we used c = 17.68 Å, with the corresponding angle of the pillar of 97.09°.

Model of pillared montmorillonite

The chemical data indicate that one Al oxy-hydroxy ion is intercalated on the average every 4.2 montmorillonite unit cells. The pillars are uniformly distributed in the interlayer (Figueras, 1988). Therefore, of 8.4 interlayer pillar sites, one site is occupied (O position) and 7.4 are vacant (V position), *i.e.*, the observed pillar-site occupancy is 11.9%.

The translational *C*-centering symmetry of the 2:1 layer requires the identical repetition of O and V positions along the [100], [$\bar{1}\bar{1}$0], and [$\bar{1}$10] directions. This is possible only if one O position alternates with the same number of V positions along each direction within a single interlayer. Figure 7 shows projections along the [001] direction of Si atoms of an adjacent 2:1 layer to the Al pillars. Three cases are shown: an alternation of one O and one V position (OVO) (Figure 7a); one O and two V positions (OVVO) (Figure 7b); and one O and three V positions (OVVVO) (Figure 7c). The three O-V alternations are described by supercells consisting of four, nine, and 16 subcells and cell parameters 2*a*, 2*b*, *c*; 3*a*, 3*b*, *c*; and 4*a*, 4*b*, *c*, respectively (Figure 7). For OVO, one pillar occupies one of four possible interlayer sites in two unit cells with a probability of 0.25. For OVVO, the pillar occupies one of nine possible positions in 4.5 unit cells with a probability of 0.111 and, for OVVVO, the pillar occupies one of 16 positions in eight unit cells with a probability of 0.0625.

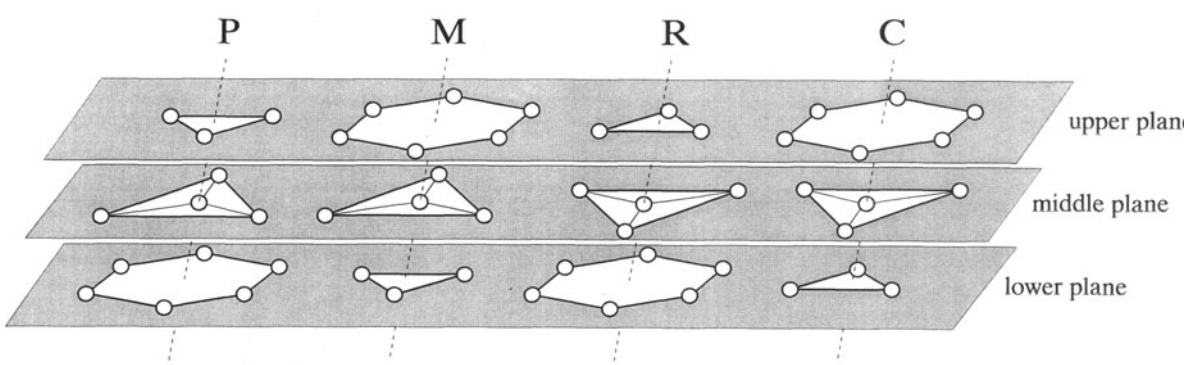

Figure 6. Different types of deformed pillars obtained by *C2/m* symmetry alteration.

https://doi.org/10.1346/CCMN.2000.0480101 Published online by Cambridge University Press

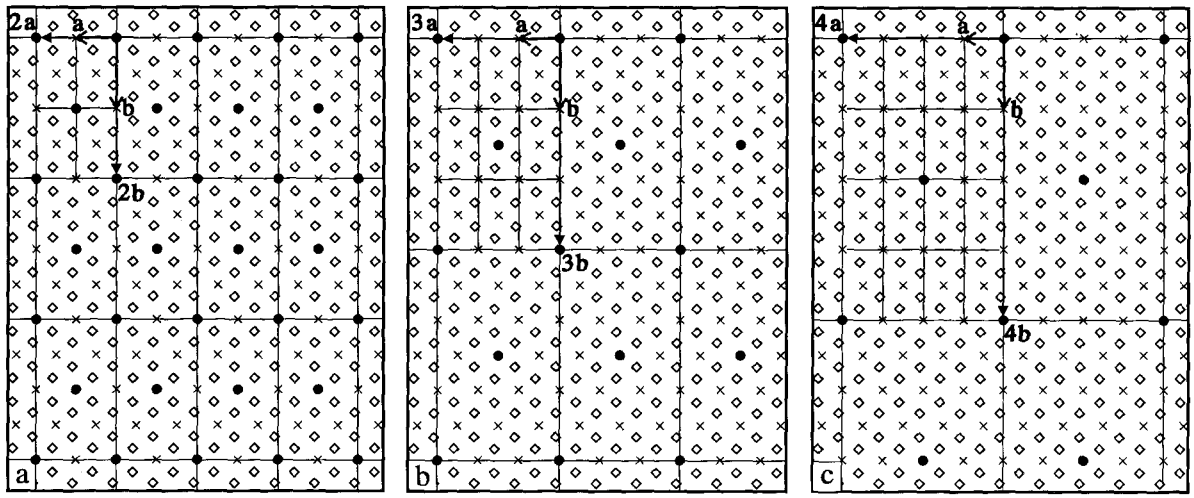

Figure 7. Mutual configuration of Al_{13} pillar and Si plane. a) OVO - 25% pillar-site occupancy; b) OVVO - 11.1% pillar-site occupancy; c) OVVVO - 6.25% pillar-site occupancy; ◊ - Si, x - V position, ● - O position.

DISCUSSION OF THE STRUCTURAL MODEL

The structure of the pillared montmorillonite may be represented by the unit cell of an enlarged interlayer montmorillonite with OVO, OVVO, or OVVVO alternating pillar layers in the interlayer. The calculated pillar-site occupancy of 11.1% of the OVVO alternation is closest to the observed pillar occupancy of 11.9% as determined from the chemical data. However, an appropriate model can represent the structure of a pillared montmorillonite with different pillar-site occupancies by choosing the correct O-V alternation.

The modeled pillar layer consists of lower, middle, and upper atomic planes (Figure 6) containing Al atoms with equal z coordinates, respectively. Figure 8 shows projections in the (001) plane of the lower, middle, and upper pillar planes. The Al positions of the P, M, C, and R pillars when they randomly occupy the O interlayer positions, are illustrated. Thirty one atomic positions may be statistically occupied by the 52 Al atoms of the four pillar types. In projection, the atomic-position arrangements in the lower and upper pillar planes are identical (Figures 6 and 8). Each of the

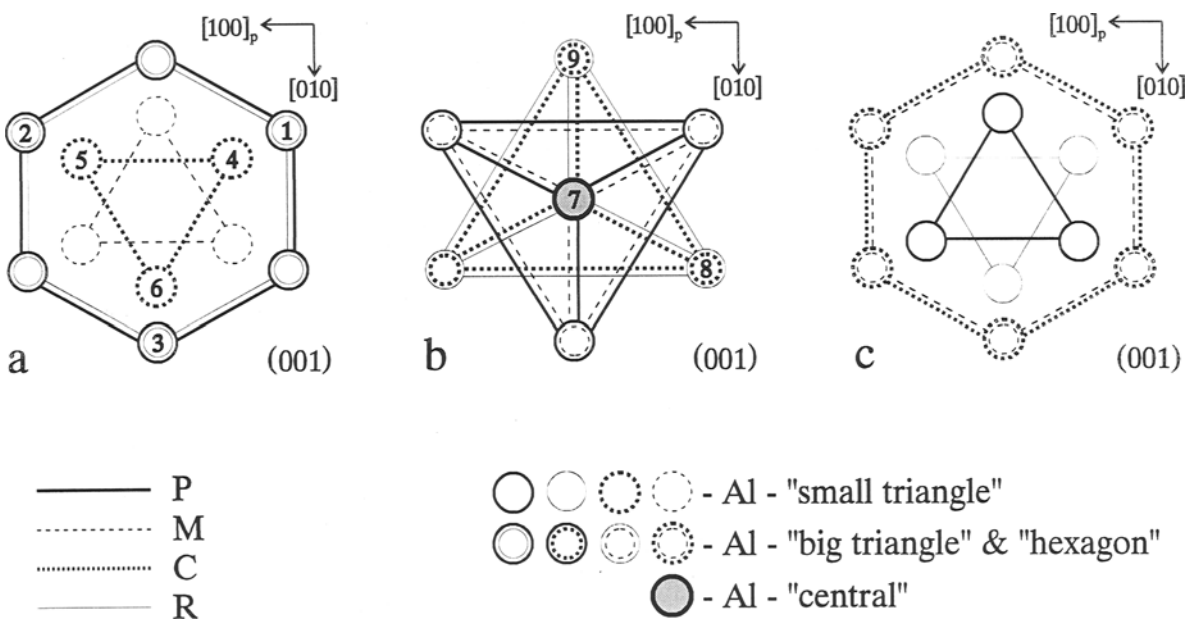

Figure 8. a) Lower, b) middle, and c) upper planes of P, R, M, and C types of pillars in (001) plane, placed alternatively in a single pillar site; the small numbers inside the Al atoms mark the symmetrically independent positions, as in Table 2b.

https://doi.org/10.1346/CCMN.2000.0480101 Published online by Cambridge University Press

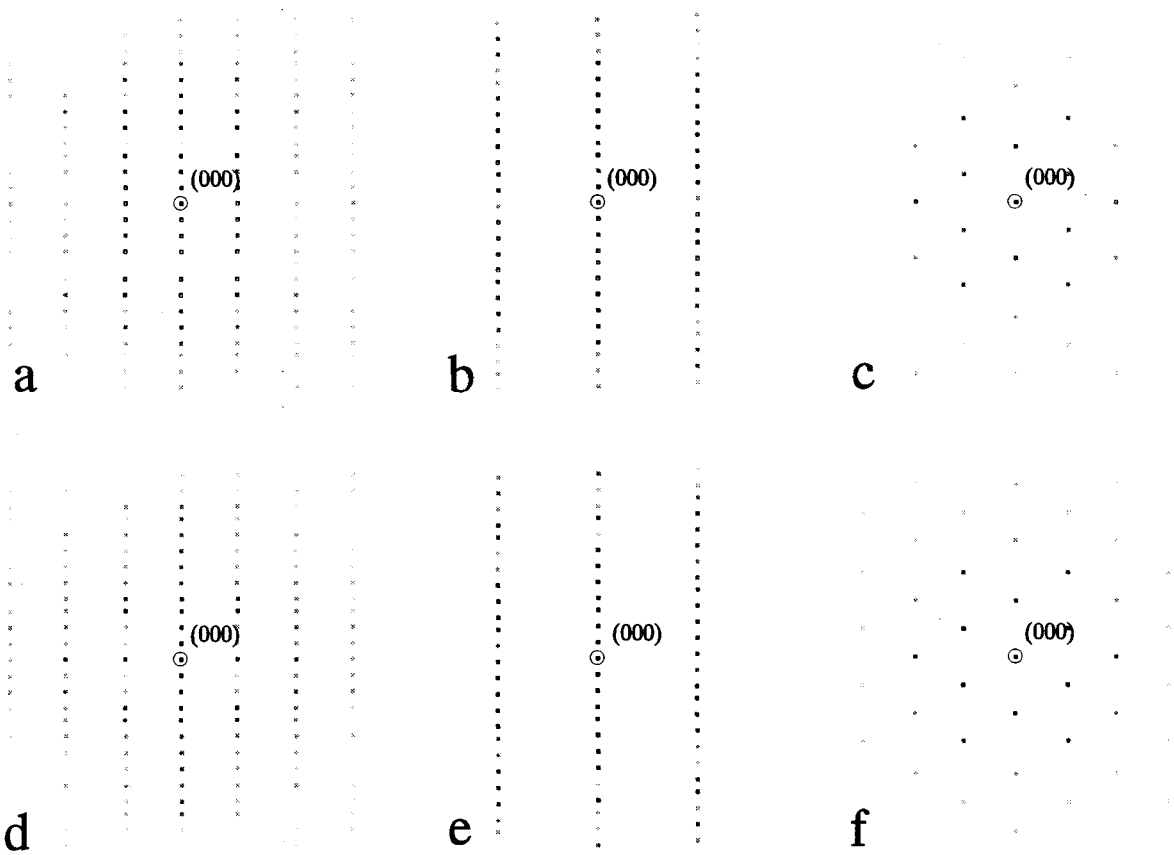

Figure 9. Simulated electron diffraction patterns along [100]*, [010]*, and [001]* directions of enlarged-interlayer (a, b, and c, respectively) and of pillared (d, e, and f, respectively) montmorillonite structures.

positions at the hexagon apices can be alternatively occupied by Al atoms from either P and R in the lower plane (Figure 8a) or M and C in the upper plane (Figure 8c), with a probable Al-site occupancy of $\frac{2}{4} = 0.5$ (**two** of the **four** possible pillars). The resultant Al-site occupancy must be the product of the pillar-site occupancy and the Al-site occupancy within the pillar. For the three O-V alternations (OVO, OVVO, OVVVO) the resultant Al-site occupancies of each of the hexagon apices are 0.125, 0.05, and 0.03125, respectively. The positions in the apices of the small triangles can be occupied by an atom from only **one** of the **four** pillar types with a probable Al-site occupancy of $\frac{1}{4} = 0.25$. The resultant Al-site occupancies of the three O-V alternations are 0.0625, 0.0277, and 0.015625, respectively.

In the middle plane (Figures 6 and 8b) the positions in the apices of the two rotated triangles can be alternatively occupied by the atoms of the C and R pillar types for one of the triangles or the P and M pillar types for the other. Each of the six positions in the apices of the two rotated triangles in the middle plane has a 0.5 Al-site occupancy to produce the same resultant Al-site occupancy as the hexagons. The position of the central Al atom of the pillar can be alternatively occupied by an Al atom from **each** of the **four** pillar types with a probable Al-site occupancy of $\frac{4}{4} = 1.0$. The resultant Al-site occupancies of this position for the three O-V alternations are respectively 0.25, 0.11, and 0.0625.

Because one montmorillonite unit cell has two symmetrically related pillar positions, there are nine symmetrically independent Al positions (Table 2b, Figure 8). The *C*2/*m* space-group symmetry then gives $31 \times 2 = 62$ possible positions alternatively occupied by the Al atoms of the four pillar types.

Single-crystal EDPs of two structural models of montmorillonite along the three coordinate axes were calculated: a) enlarged-interlayer (Figure 9a–9c) and b) pillared with resultant Al-site occupancies for the OVVO alternation (Figure 9d–9f). The patterns show the same geometry for each given direction. This confirms that the atomic structure of the modeled pillar montmorillonite retains the *C*2/*m* symmetry of the modeled enlarged-interlayer montmorillonite and respectively the *C*2/*m* symmetry of the 2:1 montmorillonite layer. However, further work is needed to obtain

https://doi.org/10.1346/CCMN.2000.0480101 Published online by Cambridge University Press

(*h*0*l*) and (0*kl*) EDPs of the pillared material for comparison.

An explanation of the increase in layer-stacking order as observed in Figure 2a *vs.* 2b may be proposed. The lower and upper atomic planes of the pillars shown in Figures 6, 8a, and 8c and their relation to the silicate rings in adjacent 2:1 layers produce a driving force for additional ordering. Two adjacent 2:1 layers may reorient as a result of rotation of the 2:1 layers and/or shift along the *a* and/or *b* axes of these layers. Assuming that the silicate rings are ideally hexagonal or trigonal, [100], [$\bar{1}\bar{1}$0], and [$\bar{1}$10] directions in two adjacent 2:1 layers may align and the EDPs of the pillared structure results in single-crystal character. The observed EDPs for the (*hk*0) plane of the pillared structure (Figure 2b) shows the same geometry as the simulated pattern (Figure 9f) but the diffraction maxima are diffuse in arcs of ~1°, probably as a result of incomplete ordering along the *c* axis.

A structural model of Al_{13}-intercalated montmorillonite developed through molecular simulation was recently reported by Čapkova *et al.* (1998). They concluded that there is no two-dimensional ordering of Al_{13} cations in the interlayers and, therefore, no regular stacking of layers can be expected in the intercalated montmorillonite. This conclusion contradicts our results. This contradiction is probably related to the different approaches to the problem under study. Our model is an attempt to explain the observed increase in the ordering along the *c* axis of the pillared montmorillonite. It is based also on literature data reporting a similar high-layer stacking order after Al_{13} pillaring of Ca-rich montmorillonites of relatively high crystallinity (*e.g.,* Storaro *et al.,* 1996). Obviously, the problem can not be unambiguously resolved since the process of pillaring is strongly clay dependent and depends also on many other factors (Schoonheydt *et al.,* 1993, 1994). In any case, we consider that modeling may be useful in resolving the structural state of the pillared clays, but each model must be based on all accessible methods of investigation and on available literature data.

ACKNOWLEDGMENTS

We thank M.P. Tarassov for the electron probe microanalysis data and the useful comments. We thank also O.E. Petrov for the critical reading of the paper and constructive discussion. This work was financially supported by the National Scientific Fund, grant Physics-332/96.

REFERENCES

Bottero, J.Y., Gases, I.M., Flessinger, F., and Poirier, J.E. (1980) Studies of hydrolysed aluminium chloride solutions. 1. Nature of Al-species and compositions of aqueous solutions. *Journal of Physics and Chemistry,* **84,** 2933–2940.

Brindley, G.W. (1980) Order-disorder in clay mineral structures. In *Crystal Structure of Clay minerals and Their X-ray Identification,* G.W. Brindley and G. Brown, eds., Mineralogical Society, London, 169–174.

Čapková, P., Driessen, A.J., Numan, M., Schenk, H., Weiss, Z., and Klika, Z. (1998) Molecular simulations of montmorillonite intercalated with aluminium complex cations. Part 1: Intercalation with $[Al_{13}O_4(OH)_{24+x}(H_2O)_{12-x}]^{(7-x)+}$, *Clays and Clay Minerals,* **46,** 232–239.

Cowley, J.M. and Moodie, A.F. (1957) The scattering of electrons by atoms and crystals: I. A new theoretical approach. *Acta Crystallographica,* **A10,** 609–619.

Figueras, F. (1988) Pillared clays as catalysts. *Catalysis Reviews: Science and Engineering,* **30,** 457–499.

Figueras, F., Klapyta, Z., Auruox, A., and Gouguen, C. (1990) Influence of the structure of the original clay on the properties of PILC materials. In *Proceedings of the International Clay Conference, Strasbourg, 1989,* V.C. Farmer and Y. Tardy, eds., Sciences Géologiques Memoire 86, 25–35.

Fijal, J. and Klapyta, Z. (1993) Heterogeneity of pillared clays. In *Proceedings of the 11th Conference on Clay Mineralogy and Petrology,* J. Konta, ed., Univerzita Karlova, Prague, 99–109.

Foster, M.D. (1953) Geochemical studies of clay minerals: II. The determination of free silica and alumina in montmorillonite. *Geochemica et Cosmochimica Acta,* **3,** 143–154.

Fripiat, J.J. (1988) High resolution solid state NMR study of pillared clays. *Catalysis Today,* **2,** 281–295.

Ilieva, A. (1996) Application of the alkylammonium exchange for layer charge determination of montmorillonites from Bulgarian bentonites. *Comptes Rendus de l'Academie Bulgare des Sciences,* **49,** 99–103.

Johansson, G. (1960) On the crystal structure of some basic aluminium salts. *Acta Chemica Scandinavica,* **14,** 771–773.

Kodama, H. and Singh, S. (1989) Polynuclear hydroxyaluminium-montmorillonite complexes: Formation of 18.8 Å and 28 Å pillared structures. *Solid State Ionics,* **32/33,** 363–372.

Occelli, M.I., Lynch, J., and Senders, J.V. (1987) TEM analysis of pillared and delaminated hectorite catalysts. *Journal of Catalysis,* **107,** 557–565.

Pinnavaia, T.J. (1983) Intercalated clay catalysts. *Science,* **220,** 365–371.

Plee, D., Gatineau, L., and Fripiat, J.J. (1987) Pillaring process of smectites with and without tetrahedral substitutions. *Clays and Clay Minerals,* **35,** 81–85.

Schönherr, S., Görz, H., and Müller, D. (1981) Herstellen und Characterisierung von $Al_{13}O_{40}Cl$-Wasserlosung. *Zeitschrift Fuer Anorganishe und Algemeine Chemie,* **476,** 188–193.

Schoonheydt, R.A. (1994) Clays: From two to three dimensions. *Studies on Surface Science and Catalysis,* **58,** 201–239.

Schoonheydt, R.A., van den Eynde, J., Tubbax, H., Leeman, H., Stuyckens, M., Lenotte, I., and Stone, W.E.E. (1993) The Al pillaring of clays. Part I. Pillaring with dilute and concentrated Al solutions. *Clays and Clay Minerals,* **41,** 598–608.

Schoonheydt, R.A., Leeman, H., Scorpion, A., Lenotte, I., and Grobet, P. (-1994) The Al pillaring of clays. Part II. Pillaring with $[Al_{13}O_4(OH)_{24}(H_2O)_{12}]^{7+}$. *Clays and Clay Minerals,* **42,** 518–526.

Storaro, L, Lenarda, M., Ganzeria, R., and Rinaldi, A. (1996) Preparation of hydroxy Al and Al/Fe pillared bentonites from concentrated clay suspensions. *Microporous Materials,* **6,** 55–63.

Tilak, D., Tennakoon, B., Jones, W., and Thomas, J.M. (1986) Structural aspects of metal-oxide-pillared sheet silicates.

Journal of the Chemical Society, Faraday Transitions 1, **82,** 3081–3095.

Tsipursky, S.I. and Drits, V.A. (1984) The distribution of octahedral cations in the 2:1 layers of dioctahedral smectites studied by oblique-texture electron diffraction. *Clay Minerals,* **21,** 187–198.

Vaughan, D.E.W. and Lussier, R.J. (1980) Preparation of molecular sieves based on pillared interlayered clays (PILC). In *Proceedings of the 5th International Conference on Zeolites, 1980,* L.V. Rees, ed., Hyden, London, 94–101.

Vaughan, D.E.W. (1988) Pillared clays—a historical perspective. *Catalysis Today,* **2,** 187–198.

E-mail of corresponding author: mincryst@bas.bg

(Received 8 August 1996; accepted 1 December 1998; Ms. 2811)